0.1 EIGENFUNCTIONS OF UNDERSPREAD LINEAR SYSTEMS: THEORY AND APPLICATIONS TO DIGITAL COMMUNICATIONS[0]

0.1.1 Summary

The knowledge of the eigenfunctions of a linear system is a fundamental issue both from the theoretical as well as from the applications point of view. Nonetheless, no analytic solution is available for the eigenfunctions of a general linear system. There are two important classes of contributions suggesting analytic expressions for the eigenfunctions of slowly-varying operators: [5], and the references therein, where it was proved that the eigenfunctions of underspread operators can be approximated by signals whose time-frequency distribution (TFD) is well localized in the time-frequency plane, and [7] where a strict relationship between the instantaneous frequency of the channel eigenfunctions and the contour lines of the Wigner Transform of the operator kernel (or Weyl symbol) was derived for Hermitian slowly-varying operators. In this article, following an approach similar to [7], we will show that the eigenfunctions can be found exactly for systems whose spread function is concentrated along a straight line and they can be found in approximate sense for those systems whose spread function is maximally concentrated in regions of the Doppler-delay plane whose area is smaller than one.

0.1.2 Eigenfunctions of time-varying systems

The input/output relationship of a continuous-time (CT) linear system is [3]:

$$y(t) = \int_{-\infty}^{\infty} h(t,\tau)x(t-\tau)d\tau \tag{0.1.1}$$

where $h(t,\tau)$ is the system impulse response. Although throughout this section we will use the terminology commonly adopted in the transit of signals through time-varying channels, it is worth pointing out that the mathematical formulation is much more general. For example, (0.1.1) can be used to describe the propagation of waves through non homogeneous media and in such a case the independent variables t and τ are spatial coordinates. Following the same notation introduced by Bello [3], any linear time-varying (LTV) channel can be fully characterized by its impulse response $h(t,\tau)$, or equivalently by the *delay-Doppler spread function* (or simply spread function) $S(\nu,\tau) := \int_{-\infty}^{\infty} h(t,\tau)e^{-j2\pi\nu t}dt$, or by the *time-varying transfer function* $H(t,f) := \int_{-\infty}^{\infty} h(t,\tau)e^{-j2\pi f\tau}d\tau$.

Since the kernels of LTV systems in general are not self-adjoint, it is not possible to define the eigenfunctions of a linear system, but we can introduce the so called *left and right singular functions* (in the following we will use the term eigenfunction

[0]Author: Sergio Barbarossa, INFOCOM Department, University of Rome "La Sapienza", Via Eudossiana 18, 00184 Rome, Italy, E-mail: sergio@infocom.uniroma1.it; Reviewers: G. Matz and A. Sayeed.

only for simplicity, meaning generically the left and right singular functions). In fact, if the system impulse response is square-integrable, i.e.

$$\int_{-\infty}^{\infty}\int_{-\infty}^{\infty}|h(t,\tau)|^2\, dt\, d\tau < \infty, \tag{0.1.2}$$

then there exists a countable set of *singular values* λ_i and two classes of orthonormal functions $v_i(t)$ and $u_i(t)$, named right and left singular functions, such that the following system of integral equations holds true

$$\lambda_i u_i(t) = \int_{-\infty}^{\infty} h(t,t-\tau)v_i(\tau)d\tau, \tag{0.1.3}$$

$$\lambda_i v_i(\tau) = \int_{-\infty}^{\infty} h^*(t,t-\tau)u_i(t)dt. \tag{0.1.4}$$

Inserting (0.1.3) in (0.1.4), we have

$$\lambda_i^2 v_i(\tau) = \int_{-\infty}^{\infty}\int_{-\infty}^{\infty} h^*(t,t-\tau)h(t,\theta)v_i(t-\theta)d\theta dt. \tag{0.1.5}$$

so that $v_i(\tau)$ is the eigenfunction of the system whose kernel is

$$\tilde{h}(\tau,\theta) := \int_{-\infty}^{\infty} h^*(t,t-\tau)h(t,t-\theta)dt. \tag{0.1.6}$$

In practice, there are at least two quite common situations where $h(t,\tau)$ is not square-integrable: i) linear time-invariant (LTI) channels, where $h(t,\tau)$ is constant along t [1]; and ii) multipath channels with specular reflections, where $h(t,\tau)$ contains Dirac pulses. However, to avoid unnecessary complications with different notations as a function of the integrability assumption, in the following we will keep assuming (0.1.2), considering the aforementioned exceptions as limiting cases, as in [4].

0.1.3 Systems with spread function confined to a straight line

If the spread function is confined to a line, i.e.

$$S(\nu,\tau) = g(\tau)\delta(\nu - f_0 - \mu\tau), \tag{0.1.8}$$

the singular functions are *chirp* signals, i.e.

$$v_i(t) = e^{j\pi\mu t^2}e^{j2\pi f_i t} \tag{0.1.9}$$

$$u_i(t) = e^{j\pi\mu t^2}e^{j2\pi f_i t}e^{j2\pi f_0 t} = v_i(t)e^{j2\pi f_0 t}. \tag{0.1.10}$$

[1] The LTI case as well as a large class of time-varying systems exhibiting some sort of stationarity can be dealt with by requiring the following integrability condition

$$\lim_{T\to\infty}\frac{1}{T}\int_{-T/2}^{T/2}dt\int_{-\infty}^{\infty}|h(t,\tau)|^2 d\tau < \infty, \tag{0.1.7}$$

instead of (0.1.2).

In fact, the impulse response corresponding to (0.1.8) is

$$h(t,\tau) = g(\tau)e^{j2\pi\mu\tau t}e^{j2\pi f_0 t} \tag{0.1.11}$$

and, substituting (0.1.11) and (0.1.9) in (0.1.3) we get

$$\lambda_i u_i(t) \; = \; e^{j2\pi f_0 t}e^{j2\pi f_i t}e^{j\pi\mu t^2}G_\mu(f_i) = G_\mu(f_i)e^{j2\pi f_0 t}v_i(t), \tag{0.1.12}$$

where $G_\mu(f)$ is the Fourier transform (FT) of $g_\mu(t) := g(t)e^{j\pi\mu t^2}$. We can verify that (0.1.12) is satisfied if $u_i(t)$ is given by (0.1.10) and $\lambda_i = G_\mu(f_i)$. It is also straightforward to check that the two classes of functions $v_i(t)$ and $u_i(t)$ are orthogonal. Interestingly, the contour lines of $|H(t,f)|$ coincide with the instantaneous frequency of the eigenfunctions. In fact, the transfer function associated to (0.1.8) is $H(t,f) = G(f-\mu t)e^{j2\pi f_0 t}$, where $G(f)$ denotes the FT of $g(\tau)$, so that $|H(t,f)|$ is constant along lines of equation $f = \mu t + f_i$, which coincides with the instantaneous frequency of the right singular functions. Furthermore, if $f_0 = 0$, i.e. $S(\nu,\tau)$ is maximally concentrated along a line passing through the origin, the left and right singular functions are simply proportional to each other and we can talk of eigenfunctions and eigenvalues. Finally, it is worth noticing that if the spread function is mainly concentrated inside a rectangle of area $B_{max}\tau_{max} \ll 1$, thus $\mu\tau_{max}^2 \ll 1$ and $|H(t, f_i + \mu t)| = |G(f_i)| \approx |G_\mu(f_i)|$, so that the modulus of the i-th eigenvalue coincides approximately with the absolute value of the channel transfer function evaluated over the curve given by the eigenfunctions' instantaneous frequency.

In the following, we will show how these results can be generalized, albeit in approximate sense, to the more challenging case where the spread function is not confined to a straight line. But, before considering the more general case, it is worthwhile to remark that the model (0.1.8) encompasses three examples of systems commonly encountered in the applications, namely i) time-invariant systems, where $S(\nu,\tau) = g(\tau)\delta(\nu)$, which corresponds to $\mu = 0$ and thus to having, as well known, sinusoidal eigenfunctions; ii) multiplicative systems, where $S(\nu,\tau) = C(\nu)\delta(\tau)$, which corresponds to $\mu = \infty$ and thus to Dirac pulses as eigenfunctions; iii) communication channels affected by *two-ray* multipath propagation, each ray having its own delay and Doppler frequency shift, i.e.

$$S(\nu,\tau) = \sum_{q=0}^{1} h_q \delta(\nu-\nu_q)\delta(\tau-\tau_q) \quad \text{or} \quad h(t,\tau) = \sum_{q=0}^{1} h_q e^{j2\pi f_q t}\delta(\tau-\tau_q). \tag{0.1.13}$$

In such a case, the eigenfunctions are chirp signals having different initial frequencies, but all with the same sweep rate $\mu = (f_1 - f_0)/(\tau_1 - \tau_0)$, which depends on the channel delay and Doppler parameters.

0.1.4 Analytic models for the eigenfunctions of underspread channels

We extend now the analysis to systems whose spread function has a support, in the delay-Doppler domain, with small, but, differently from the previous case, non-null area. Interestingly, this case encompasses all current digital communication systems. The aim of the ensuing analysis is to show that if $S(\nu,\tau)$ is mainly concentrated around the origin of the Doppler-delay plane, along one of the two axes but not along both, the main result derived above can be generalized, even though only in approximate sense.

First of all, proceeding as in [5], we define the absolute moments of $S(\nu,\tau)$ as

$$m_S^{(k,l)} := \frac{\int_{-\infty}^{\infty}\int_{-\infty}^{\infty}|\nu|^k|\tau|^l|S(\nu,\tau)|d\nu d\tau}{\int_{-\infty}^{\infty}\int_{-\infty}^{\infty}|S(\nu,\tau)|d\nu d\tau}. \tag{0.1.14}$$

We say that a system is *underspread* if all the products $m_S^{(i,j)}m_S^{(k,l)}$ of order $i+j+k+l \geq 2$, where the indices are such that there is at least the product of a non null moment along τ times a non null moment along ν, are "small". This definition is not rigorous, but its meaning will be clarified within the proof of the main statement of this section. Since the partial derivatives of $H(t,f)$ can be upper bounded as follows

$$\left|\frac{\partial H^{k+l}(t,f)}{\partial t^k \partial f^l}\right| \leq (2\pi)^{k+l} m_S^{(k,l)} \int_{-\infty}^{\infty}\int_{-\infty}^{\infty}|S(\nu,\tau)|d\nu d\tau, \tag{0.1.15}$$

if $S(\nu,\tau)$ has small moments, $H(t,f)$ must be a *smooth function* in at least one direction.

In the following we show that, if the system is underspread, the singular function associated to the i-th singular value can be approximated by the following analytic function

$$v_i(t) := \sum_{m=1}^{K_i(t)} v_{i,m}(t) := \sum_{m=1}^{K_i(t)} a_{i,m}(t)e^{j\phi_{i,m}(t)}, \tag{0.1.16}$$

where i) the instantaneous phase $\phi_{i,m}(t)$ is such that the corresponding instantaneous frequency $f_{i,m}(t) := \dot{\phi}_{i,m}(t)/2\pi$ of $v_{i,m}(t)$ is one of the real solutions of

$$|H(t,f_{i,m}(t))|^2 = \lambda_i^2, \quad \forall m; \tag{0.1.17}$$

ii) the amplitude $a_{i,m}(t)$ is approximately constant and different from zero only within the time interval where $|H(t,f_{i,m}(t))|^2 = \lambda_i^2$ admits a real solution, and its value is such that $v_i(t)$ has unit norm; $K_i(t)$ is the number of solutions of (0.1.17), for each λ_i and t.

The existence of a real solution for $f_{i,m}(t)$ of (0.1.17) implies that the singular values λ_i must be bounded in the following interval: $\min_{t,f}|H(t,f)| \leq \lambda_i \leq \max_{t,f}|H(t,f)|$. Between these two boundaries, not all values of λ_i are possible: The only admissible values are the ones that allow the eigenfunctions to be orthonormal and respect Heisenberg's uncertainty principle, similarly to the area rule suggested in [7].

From (0.1.17) we notice that the instantaneous frequencies of the system eigenfunctions coincide with the contour lines of $|H(t,f)|$. Typically, the contour plots are closed curves and then $K_i(t)$ is usually an even integer. In general, we have verified numerically that if there are more closed curves corresponding to the same eigenvalue λ_i, the multiplicity of the eigenvalue is equal to the number of closed curves corresponding to λ_i, with each closed curve giving rise to one eigenfunction.

We show now under which approximations, the function $v_i(\tau)$, as given in (0.1.16), is a solution of (0.1.5). Exploiting the system linearity, we compute the output $y_{i,m}(t)$ corresponding to each m-th component $v_{i,m}(t)$ in (0.1.16) and then we exploit the superposition principle to derive the output corresponding to $v_i(t)$. In our proof, we assume that the support of $h(t,\tau)$ along τ is small[2]. As a consequence, for each value of τ, the product $h^*(t,t-\tau)h(t,\theta)$ in (0.1.5) assumes significant values only for small values of both $t-\tau$ and θ. We can thus expand $v_{i,m}(t-\theta)$ in (0.1.5), around τ and keep only the lower order components

$$v_{i,m}(t-\theta) \approx a_{i,m}(\tau)e^{j\phi_{i,m}(\tau)}e^{j\dot{\phi}_{i,m}(\tau)(t-\theta-\tau)}, \tag{0.1.18}$$

having used a first order approximation for $\phi_{i,m}(t-\theta)$ and a zero-th order approximation for $a_{i,m}(t-\theta)$. Substituting (0.1.18) into (0.1.5) and invoking the principle of stationary phase [6] to derive an approximate analytic expression of the integral, we get the m-th output term

$$\begin{aligned} y_{i,m}(\tau) &\approx a_{i,m}(\tau)e^{j\phi_{i,m}(\tau)}\int_{-\infty}^{\infty}\int_{-\infty}^{\infty} h^*(t,t-\tau)h(t,\theta)e^{-j\dot{\phi}_{i,m}(\tau)\theta}e^{j\dot{\phi}_{i,m}(\tau)(t-\tau)}d\theta dt \\ &= a_{i,m}(\tau)e^{j\phi_{i,m}(\tau)}\int_{-\infty}^{\infty} h^*(t,t-\tau)H(t,f_{i,m}(\tau))e^{j\dot{\phi}_{i,m}(\tau)(t-\tau)}dt. \end{aligned} \tag{0.1.19}$$

After a few algebraic manipulations involving the Taylor's series expansion of both $h(t,t-\tau)$ and $H(t,f)$ around τ in their first argument and summing over m, we get

$$y(\tau) \approx \lambda_i^2 v_i(\tau) + \sum_{m=1}^{K_i}\underbrace{\sum_{k,l=0}^{\infty}}_{k,l\neq 0}\frac{H_{t,f}^{(k,0)}(\tau,f_{i,m}(\tau))H_{t,f}^{(l,k+l)^*}(\tau,f_{i,m}(\tau))}{(-j2\pi)^{k+l}k!\,l!}a_{i,m}(\tau)e^{j\phi_{i,m}(\tau)}, \tag{0.1.20}$$

where $H_{t,f}^{(k,l)}(t,f) := \partial^{k+l}H(t,f)/\partial t^k\partial f^l$. This equation shows that $v_i(\tau)$, as given in (0.1.16), is (approximately) the eigenfunction associated to the eigenvalue λ_i^2 if the perturbation, given by the second term of the right-hand side of (0.1.20), is small with respect to $\lambda_i^2 v_i(\tau)$. From (0.1.20), we notice that the perturbation is equal to the sum of complex functions given by the product of the partial derivatives of the system transfer function, evaluated along the curve where the modulus of the transfer function is constant. Furthermore, each term in the perturbation contains

[2]If this assumption is not true, to respect our main assumption about the concentration of the spread function, the spread of $S(\nu,\tau)$ along ν must be very small. In such a case, using duality arguments, we can derive equivalent results working with the spectrum of the eigenfunctions.

at least the first order derivative with respect to both time and frequency. Therefore, the perturbation is small with respect to the first term in (0.1.20) if the transfer function is smooth in at least one direction, i.e. time or frequency. Hence, the analytic model (0.1.16) is valid only for underspread systems, i.e. systems whose transfer function has small partial derivatives, by virtue of (0.1.15), in at least one direction. Furthermore, since the energy of the first term is λ_i^4, the approximation error is smaller for the highest eigenvalues.

Since so many approximations have been used to justify the analytic model (0.1.16), it is necessary to check the validity of such approximations. Given the crucial role played by the instantaneous frequency in the definition of the system eigenfunction and the interplay of time and frequency, the analysis of the time-frequency distribution (TFD) of the system eigenfunctions plays a fundamental role as a validation tool. Since the validation is necessarily numerical, we start deriving the equivalent discrete-time (DT) system corresponding to the continuous-time (CT) relationship (0.1.1). Specifically, we consider the system obtained by windowing $h(t,\tau)$ in time and in frequency. Assuming that the input signal $x(t)$ has a spectrum confined within the bandwidth $[-1/2T_s, 1/2T_s]$, we can express $x(t)$ as

$$x(t) = \sum_{k=-\infty}^{\infty} x[k]\mathrm{sinc}(\pi(\mathrm{t}-\mathrm{kT_s})/\mathrm{T_s}), \tag{0.1.21}$$

where $x[k] := x(kT_s)$ and$1/T_s$ is the sampling rate. Sampling the continuous time system output $y(t)$ at the same rate $1/T_s$[3], we get the equivalent discrete-time I/O relationship

$$y[n] := y(nT_s) = \sum_{k=-\infty}^{\infty} h[n, n-k]x[k], \tag{0.1.22}$$

where $h[n,k]$ denotes the equivalent DT impulse respeonse, defined as

$$h[n, n-k] := \int_{-\infty}^{\infty}\int_{-\infty}^{\infty} \mathrm{sinc}(\pi(\mathrm{nT_s}-\theta)/\mathrm{T_s})\mathrm{sinc}(\pi(\theta-\tau-\mathrm{kT_s})/\mathrm{T_s})\mathrm{h}(\theta,\tau)\mathrm{d}\tau\mathrm{d}\theta. \tag{0.1.23}$$

Equation (0.1.22) is the DT counterpart of (0.1.1). Assuming that $h[n,k]$ has finite support over k, i.e. the channel is FIR of order L, and parsing the input sequence into consecutive blocks of size R, the discrete-time model leads directly to the matrix I/O relationship $\boldsymbol{y}(n) = \boldsymbol{H}(n)\boldsymbol{x}(n)$, where $\boldsymbol{H}(n)$ is the $P \times R$ channel matrix, with $P = R + L$, relative to the n-th transmitted block, whose (i,j) entry is $\{\boldsymbol{H}(n)\}_{i,j} = h[nP+i, i-j]$, whereas $\boldsymbol{x}(n) := (x[nR], \ldots, x[R+R-1])^T$ and $\boldsymbol{y}(n) := (y[nP], \ldots, y[nP+P-1])^T$ are the input and output blocks.

The discrete time counterpart of (0.1.3) and (0.1.4) is the singular value decomposition (SVD) of the channel matrix $\boldsymbol{H}(n)$, i.e. $\boldsymbol{H}(n) = \boldsymbol{U}(n)\boldsymbol{\Lambda}(n)\boldsymbol{V}^H(n)$, that

[3]We assume that $1/T_s$ is large enough to respect the Nyquist principle for the system output $y(t)$; this means that, if we take into account the bandwidth increase due to the transit through a time-varying system, $1/T_s$ is strictly larger than the bandwidth of $x(t)$.

allows us to write

$$\boldsymbol{U}(n)\Lambda(n) = \boldsymbol{H}(n)\boldsymbol{V}(n), \quad or \quad \boldsymbol{H}^H(n)\boldsymbol{U}(n) = \boldsymbol{V}(n)\boldsymbol{\Lambda}(n), \tag{0.1.24}$$

where the columns of $\boldsymbol{U}(n)$ and $\boldsymbol{V}(n)$ are the left and right channel singular vectors associated to the singular values contained in the diagonal matrix $\boldsymbol{\Lambda}(n)$.

To check the validity of model (0.1.16), we proceed through the following steps. Given the impulse response $h(t,\tau)$ of the CT system, i) we build the channel matrix $\boldsymbol{H}(n)$ of the equivalent DT system; ii) we compute the SVD of $\boldsymbol{H}(n)$; iii) we compute the TFD of the right and left singular vectors associated to the generic singular value λ_i; and iv) we compare the energy distribution of these TFD with the contour plot of $|H(t,f)|$ corresponding to level λ_i. We used as a basic tool to analyze the signals in the time-frequency domain the Smoothed Pseudo-Wigner-Ville Distribution (SPWVD) with reassignment, introduced in [1], for its property of having low cross terms without degrading the resolution. We considered as a test system a communication channel affected by multipath propagation, thus described by the CT impulse response

$$h(t,\tau) = \sum_{q=0}^{Q-1} h_q e^{j2\pi f_q t}\delta(\tau - \tau_q),$$

where each path is characterized by the triplet of amplitude h_q, delay τ_q and Doppler shift f_q. We generated the amplitudes h_q as independent identically distributed (iid) complex Gaussian random variables with zero mean and unit variance (the Rayleigh fading model), and the variables τ_q and f_q as iid random variables with uniform distribution within the intervals $[0,\Delta\tau]$ and $[-\Delta f/2, \Delta f/2]$, respectively. An example, relative to a multipath channel composed of $Q = 12$ paths, with $\Delta\tau = 4T_s$ and $\Delta f = 4/NT_s$, $N = 128$, is reported in Fig. 1 where we show: a) the mesh plot of $|H(t,f)|$, b) two contour plots of $|H(t,f)|$ corresponding to the levels λ_{16} (dashed line) and λ_{32} (solid line); c) the contour plot of the SPWVD of $\boldsymbol{v}_{16}$; d) the contour plot of the SPWVD of $\boldsymbol{v}_{32}$.

It is worth noticing how, in spite of the rather peculiar structure of the contour plots of $|H(t,f)|$, the SPWVD's of the two singular functions are strongly concentrated along curves coinciding with the contour lines of $|H(t,f)|$ corresponding to the associated singular values, as predicted by the theory.

It is also interesting to observe the *bubble*-like structure of the two SPWVD's. Indeed this behavior is quite common, because in general the contour lines of the time-varying transfer function are typically closed curves.

Before concluding this section, it is also important to provide some physical insight to justify the rather peculiar behavior of the channel eigenfunctions. Indeed, the bubble-like structure is perfectly functional to guaranteeing two of the fundamental properties of the eigenfunctions, namely orthogonality and system modes excitation. In fact, by construction, (0.1.16) and (0.1.17) insure that the instantaneous frequency curves of singular functions associated to distinct eigenvalues do not intersect. Therefore, if the WVD's of the eigenfunctions associated to distinct

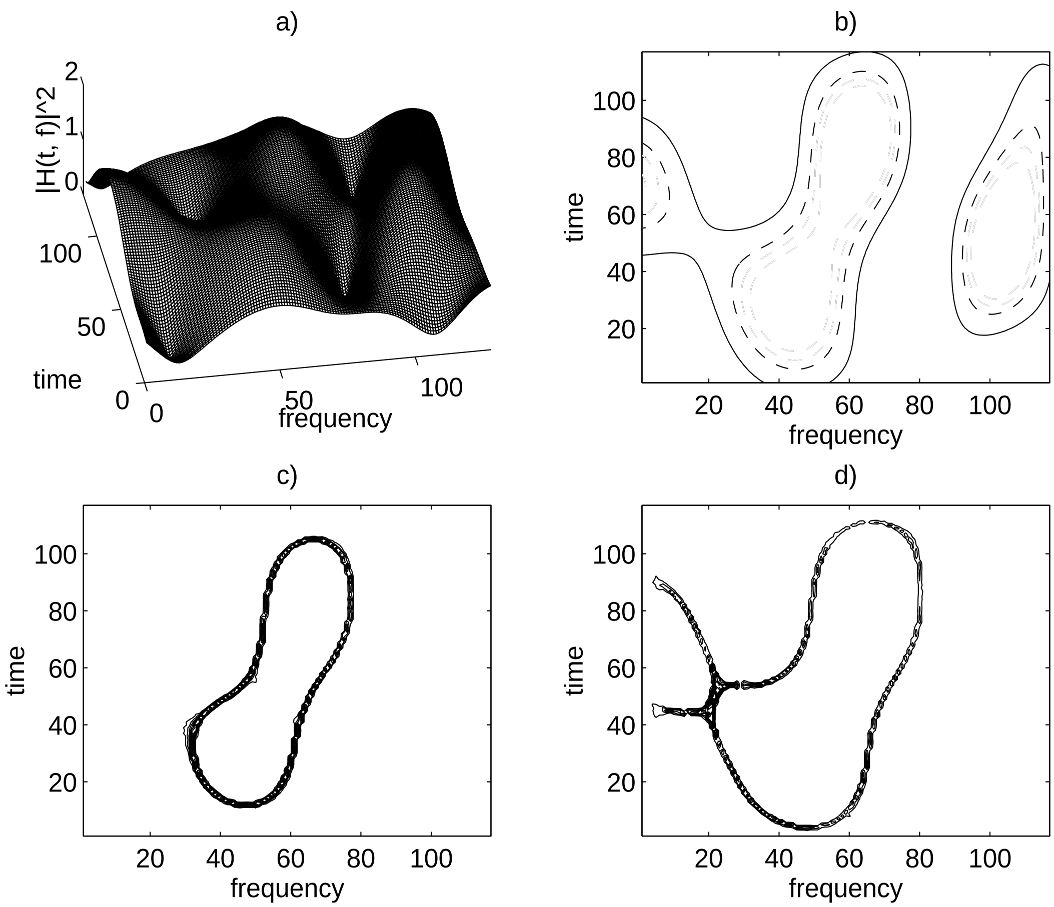

Figure 1: Comparison between contour lines of $|H(t,f)|$ and TFD's of channel singular vectors - a) $|H(t,f)|$; b) contour lines of $|H(t,f)|$ corresponding to levels λ_{16} (dashed line) and λ_{32} (solid line); c) SPWVD of $\boldsymbol{v}_{16}$; d) SPWVD of $\boldsymbol{v}_{32}$.

eigenvalues are well concentrated along their instantaneous frequency curve (i.e. if their amplitude modulation is negligible), the scalar product of their WVD's is null and thus, by virtue of Moyal's formula, the eigenfunctions are orthogonal, as required. Considering now the modes of the system, we know that the unit energy input signal that maximizes the output energy is the right singular function associated to the highest singular value. Now, if we combine this basic property with the model given in (0.1.16) and (0.1.17), we can conclude that, not surprisingly, the input signal which maximizes the output energy is the signal whose energy is concentrated in the time-frequency region where the channel time-varying transfer function is maximum.

0.1.5 Optimal waveforms for digital communications through LTV channels

Let us consider one of the most interesting applications of the theory described above, i.e. the transmission of information symbols $s[k]$ through an LTV channel. In Article 13.2, for example, it is shown how to convert the channel dispersiveness, possibly in both time and frequency domains, into a useful source of diversity to be exploited to enhance the SNR at the receiver. Here we show that if the transmitter is able to predict the channel time-varying transfer function, at least within the next time slot where one is going to transmit, it is possible to optimize the transmission strategy and take full advantage of the diversity offered by the channel dispersiveness (see e.g. [2] for more details).

Considering a channel with approximately finite impulse response of order L, we can parse the input sequence in consecutive blocks of K symbols and insert null guard intervals of length L between successive blocks to avoid inter-block interference. If the symbol rate is $1/T_s$, the time necessary to transmit each block is KT_s. For each i-th block, we must consider the channel $h_i(t,\tau)$ obtained by windowing $h(t,\tau)$ in time, in order to retain only the interval $[iKT_s,(i+1)KT_s]$, and in frequency, keeping only the band $[-1/2T_s, 1/2T_s]$. The optimal strategy for transmitting a set of symbols $s_i[k] := s[iK+k]$, $k=0,\ldots,K-1$, in the presence of additive white Gaussian noise (AWGN), is to send the signal [4]

$$x_i(t) = \sum_{k=0}^{K-1} c_{i,k} s_i[k] v_{i,k}(t) \tag{0.1.25}$$

where $v_{i,k}(t)$ is the right singular function associated to the k-th eigenvalue of the channel response $h_i(t,\tau)$ in the i-th transmit interval and $c_{i,k}$ are coefficients used to allocate the available power among the transmitted symbols according to some optimization criterion [2]. Using (0.1.3), the received signal is thus

$$y_i(t) = \int_{-\infty}^{\infty} h_i(t,\tau)x_i(t-\tau)d\tau + w(t) = \sum_k c_{i,k}\lambda_{i,k}s_i[k]u_{i,k}(t) + w(t), \tag{0.1.26}$$

where $u_{i,k}(t)$ is the left singular function associated to the k-th singular value of $h_i(t,\tau)$ and $w(t)$ is AWGN. Hence, by exploiting the orthonormality of the functions $u_{i,k}(t)$, the transmitted symbols can be estimated by simply taking the scalar products of $y(t)$ with the left singular functions, i.e.

$$\hat{s}_i[m] = \frac{1}{\lambda_{i,m} c_{i,m}} \int_{-\infty}^{\infty} y(t) u_{i,m}^*(t) dt = s[m] + w_i[m], \qquad (0.1.27)$$

where the noise samples sequence $w_i[m] := \int_{-\infty}^{\infty} w(t) u_{i,m}^*(t) dt$ constitutes a sequence of iid Gaussian random variables. In this way, the initial LTV channel, possibly dispersive in both time and frequency domains, has been converted into a set of parallel independent non-dispersive subchannels, with no intersymbol interference, and the symbol-by-symbol decision is also the maximum likelihood detector.

Most current transmission schemes turn out to be simple examples of the general framework illustrated above. For example, in communications through flat fading multiplicative channels, whose eigenfunctions are Dirac pulses, the optimal strategy is time division multiplexing. By duality, the optimal strategy for transmitting through linear time-invariant channels is orthogonal frequency division multiplexing (OFDM). Interestingly, in the most general case (of underspread channels), the optimal strategy consists in sending symbols through channel-dependent *bubble-carriers*.

0.1.6 Conclusion

The analytic model for the eigenfunctions of underspread linear operators shown in this article, albeit approximate, shows that the energy of the system eigenfunctions is mainly concentrated along curves coinciding with the level curves of the system transfer function. This property, for whose validation the analysis of the system eigenfunctions' TFD plays a fundamental role, provides a general framework to interpret some current data transmission schemes and, most important, gives a new perspective to envisage the optimal waveforms for transmissions over time-varying channels.

Pictorially speaking, if we draw a parallelism between time-frequency representations and musical scores, we may say that the eigenfunctions of underspread systems give rise to a polyphonic texture which reduces to monophonic lines only in the simple case of systems whose spread function is concentrated on a straight line. In the most general case, we have a polyphony of ascending and descending melodical lines which run in order to create bubbles whose shape is dictated by the contour lines of the system transfer function.

References

[1] F. Auger and P. Flandrin, "Improving the Readability of Time-Frequency and Time-Scale Representations by the Reassignment Method", *IEEE Trans. on Signal Proc.*, Vol.43, No.5, May 1995, pp.1068-1089.

[2] S. Barbarossa, A. Scaglione, "Time-Varying Fading Channels", in *Signal Processing Advances in Wireless and Mobile Communications - Trends in Single and Multi-User Systems*, (Ed. by G. B. Giannakis, Y. Hua, P. Stoica, and L. Tong), Vol. 2, Prentice-Hall, 2001.

[3] P.A. Bello,“Characterization of randomly time-variant linear channels”, *IEEE Trans. on Circuits and Systems*, vol. CS-11, No. 4, pp. 360–393, Dec. 1963.

[4] R. Gallager, *Elements of Information Theory*, Section 8, New York: Wiley, 1968.

[5] G. Matz, F. Hlawatsch “Time-Frequency Transfer Function Calculus (Symbolic Calculus) of Linear Time-Varying Systems (Linear Operators) Based on a Generalized Underspread Theory”, *Journal of Mathematics Physics* (Special issue on Wavelets and Time-Frequency Analysis), vol. 39, no. 8, pp.4041-4070, Aug. 1998.

[6] A. Papoulis, *Signal Analysis*, McGraw Hill, New York, 1977.

[7] L. Sirovich, B. W. Knight, “On the eigentheory of operators which exhibit a slow variation”, *Quart. Appl. Math.*, Vol. 38, pp. 469-488, 1980.